*31st EPS Conference on Plasma Phys. London, 28 June - 2 July 2004 ECA Vol.**28G**, P-1.128 (2004)*

Observation of DED–induced Magnetic Islands by a Tangentially Viewing Soft X–ray Camera on the TEXTOR Tokamak

S. Ohdachi[1], G. Fuchs, G. Bertschinger, K. H. Finken, K. Toi[1] and Textor Team

Institut für Plasmaphysik, Forschungszentrum Jülich GmbH,
EURATOM Association, D–52425 Jülich, Germany
[1] *National Institute for Fusion Science, Toki–shi 509–5292, Japan*

1 Introduction

Generation and evolution of the magnetic islands in magnetically confined plasmas attract wide interests. Magnetic islands play an important role in the confinement and stability of fusion plasmas. For example, the neo–classical tearing mode grows from seed islands, which are produced by small disturbances, and may limit the performance of tokamak plasmas. A tangentially viewing camera is suitable to study the dynamics of the magnetic islands. Since the magnetic islands extend toroidally along the magnetic field lines, they can be visualized better when they are observed tangentially. Thereby, we can study the evolution of structures of islands with higher spatial resolution.

A fast framing tangentially viewing soft X–ray camera system [1] used in Large Helical Device was installed on the TEXTOR-94 tokamak in the last experimental campaign. It can record soft X-ray (E > 1keV) images of the plasma with a framing rate of 4.5kHz (full–frame mode) and 13.5kHz (half–frame mode).

In this study, we describe a practical way to treat this kind of two-dimensional fluctuation data using singular value decomposition (SVD) . To investigate coherent modes, e.g. MHD instabilities, FFT based analysis acts as a tool that expands signals by trigonometric functions. The SVD method works similar, however, it uses an expansion to orthogonal but otherwise arbitrary functions. By SVD, a matrix A made up of n time series of m frames is decomposed into three matrices U, V and a diagonal matrix W such that $A = UWV^t$. The columns of U and V are spatial and temporal orthogonal vectors and are called Topos and Chronos, respectively. A time series $\boldsymbol{a}_i$ can be written by a combination of orthogonal components of the Topos and the Chronos type

$$\boldsymbol{a}_i = w_1 \times v_{i1} \times \boldsymbol{u}_1 + w_2 \times v_{i2} \times \boldsymbol{u}_2 + \cdots + w_m \times v_{im} \times \boldsymbol{u}_m. \quad (1)$$

Here, w_i^2 is a measure of the contribution from a particular component to the total fluctuation power. In practice, a few of the larger components suffice to describe the nature of the fluctuations, meaning that we may interpret the data using a small number of orthogonal components only.

To analyze two–dimensional line–integrated data, we might proceed as follows; first we perform tomographic reconstructions of the images, then we analyze the result with the SVD method. However, this requires much CPU power and noise is amplified by the inversion process. Therefore, we adopt another strategy; first we make a SVD analysis, then we do reconstruction to arrive at the result. As SVD and Radon transform are both linear operations, they commute and one can reconstruct the local pictures from the Topos only [2]. In the following section, we will perform the direct SV decomposition of the images. We will analyze the images obtained in 3/1 mode DED experiments on TEXTOR tokamak [3] in the section 3.

2 Tomographic reconstruction for tangentially viewing camera system

From one tangential view of the plasma, it is not possible to reconstruct a three-dimensional radiation profile. We assume that radiation along the magnetic field lines is constant and try to re-

construct a two-dimensional profile on a poloidal plane. A column vector $\boldsymbol{S}(S_i = 1, 2, \ldots, M)$ representing measured signals or Topos can be expressed as a linear combination of the radiation profile $\boldsymbol{E}$ $(E_i = 1, 2, \ldots, K)$ and the residual error vector $\boldsymbol{e}$, $\boldsymbol{S} = L\boldsymbol{E} + \boldsymbol{e}$.

The geometrical weight matrix L (M×K)) can be determined from integration along the line of sight (Fig. 1). We assume that the magnetic flux surfaces are circular and are shifted by $\Delta = \Delta_0(1-\rho^2)$, $(\rho = r/a)$ (Fig.1.(c)). Thereby all elements along a line of sight can be connected to elements in the reference poloidal plane (P2 in Fig. 1) by magnetic field lines(Red / Blue lines in Fig. 1). We assume the q–profile to be, $q(\rho) = \rho^2/(1-(1-\rho^2)^{(q_a+1)})\, q_a$. In this study, M ~ 2500 (effective channels looking at plasma within 64 ×64 pixels in the detector) and K = 1024 (poloidal cross section of the plasma is divided by 32 × 32). Since the reconstruction from the tangential view is an ill–posed problem, the least square solution of the equation is rather unstable; we need some smoothing mechanism or regularization. We make use of two methods. One is standard Fourier-Bessel (FB) expansion [4]. The radiation profile $\boldsymbol{E}$ is assumed to be in the form $\sum_{m=0}^{\infty}\sum_{l=0}^{\infty} a_{ml}\exp(im\theta)J_m(\lambda_m^l\rho)$. The coefficients a_{ml} will be determined by a least square fit. Here, J_m is the m th order Bessel function and λ_m^l is the ł th zero–point of J_m. If we cut higher modes, this fitting will act as smoothing. The other method is Phillips-Tikhonov (PT) regularization[5, 6]. In this scheme, minimization of

$$Q = \gamma \sum |C\boldsymbol{E}|^2 + \frac{1}{M}\sum |\boldsymbol{S} - L\boldsymbol{E}|^2. \tag{2}$$

is considered rather than minimizing $\sum |\boldsymbol{S} - L\boldsymbol{E}|^2$ itself. The matrix C acts as Laplacian operator. The first term of the Eq. 2 decreases when the radiation profile is smoothed; parameter γ acts as the control parameter of the profile smoothness. After the matrix $C^{-1}L$ is SV decomposed as UWV^t,

$$\boldsymbol{E}(\gamma) = \sum_{j=1}^{p} w_j(\gamma)\frac{\boldsymbol{u}_j \cdot S}{\sigma_j}(C^{-1}\boldsymbol{v}_j). \tag{3}$$

$\boldsymbol{E}$ is now written as combination of orthogonal patterns $C^{-1}\boldsymbol{v}_j$ (Fig. 2) with weighing factors $w_j(\gamma) = 1/(1 + M\gamma/\sigma_j^2)$. w_j is a decreasing function of j and the destabilizing effect from the small-scale structure (higher j components) is suppressed by proper choice of γ. Each of the schemes has its own merits and drawbacks. In BF expansion, radiation at the last closed flux surface is automatically set to zero. It is useful to avoid 'GHOSTS' near the plasma edge. With the PT method, we do not need to make assumptions about the shape of the flux surfaces; this will be useful when we want to analyze relaxation phenomena, e.g. sawteeth in tokamaks.

The reconstructions by both methods are shown in Fig. 3. Quite similar radiation profiles are obtained from the measurements. In FB inversion, poloidal mode $0 \le m \le 6$ and radial mode $0 \le l \le 9$ are included. In PT inversion, $\gamma = 1.0$ is used. In the references, the minimum of Akaike's Information Criterion (AIC) for FB and Generalized Cross Validation (GCV) for PT was used to determine the number of the free parameters. However, in our case, no clear minimum has been found. We took the point where the gradient of AIC / GCV starts to decrease as the number of the parameter increases.

3 DED experiments and the m=2 island structures

A dynamic ergodic divertor has been implemented on TEXTOR tokamak to control the heat fluxes in the edge region. The DED coil system is located on the high-field side of TEXTOR; external perturbation fields with poloidal / toroidal mode numbers m/n = 12/4, 6/2, 3/1 can be applied. When a co-rotating (1kHz) 3/1 perturbation field, which penetrates deeper into the plasma than a 12/4 field, is used, a rotating structure with the same frequency as the applied field is detected. Four SVD components are shown in Fig. 4. Obviously, the first Topo (A0) represents the global change of the whole

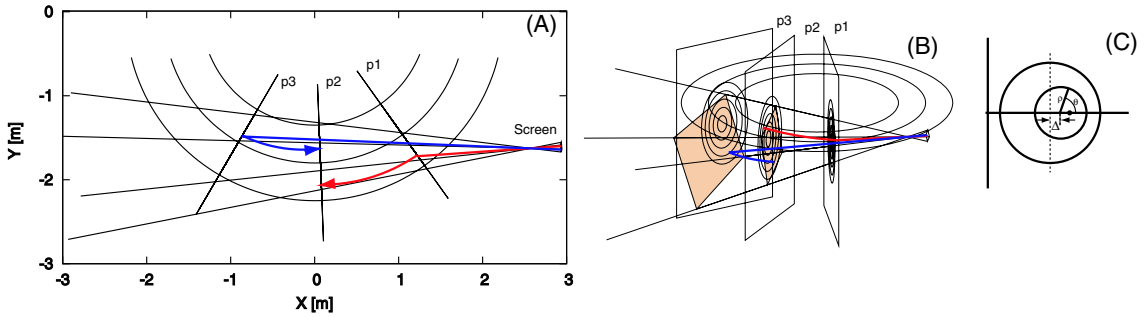

Fig.1: Geometry of the tangentially viewing camera system. On the equatorial plane (A) and the bird-view diagram (B) are shown. To project images on the plane (p2) we assume a magnetic flux shifted by $\Delta(\rho) = \Delta_0(1-\rho^2)$ shown in (C).

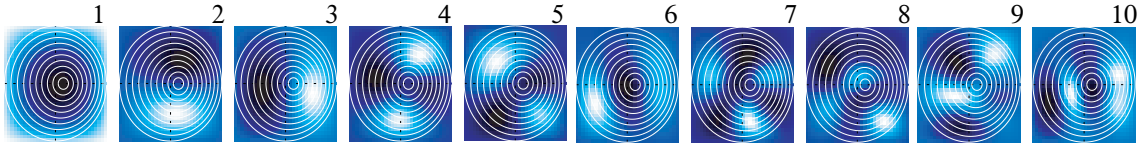

Fig.2: First ten orthogonal patterns of TP method in this geometry.

plasma shape. Choronos B2, B3 are synchronized with the external DED coil currents, the phases are different. For Topos A2, A3, we recognize that it is a rotation of the structure. Reconstructed images for B2, B3 are shown in C2, C3. There are m = 2 structures around $\rho \sim 0.5$ in both components and m = 3 structure around $\rho \sim 0.7$ can be seen in C3. The radial width of these structure is about 10 ~ 15 % of the minor radius. These rotating modes can be seen when the DED current exceeds a certain threshold. In some cases m = 2 structures remain after the DED current is terminated (cf [7]). The shape of these structures is similar to those during the external perturbation.

4 Conclusion

With SVD based analysis, we can effectively detect island-like structures in DED 3/1 mode experiments. Because the data of our diagnostics are incomplete in two aspects; outer part of the plasma cross section– mainly on the low field side– is not seen, and we have a 2–dimensional view only. The inversion is prone to errors, therefore, there is a need to compare with other diagnostics. We started this comparison, however, more detailed work will be needed

References

[1] S. Ohdachi *et al.*, Rev. Sci. Instrum **74**, (2003).

[2] G. Fuchs, Y. Miura, and M. Mori, Plasma Phys. Control. Fusion **36**, 307 (1994).

[3] K. H. Finken, Nucl. Fusion **37**, 583 (1997).

[4] Y. Nagayama, J. Appl. Phys. **62**, 2702 (1987).

[5] N. Terasaki, N. Iwama, and Y. Hosoda, The Transaction of the Institute of Electronics, Information and Communication Engineers D-II (in Japanese) **81**, 93 (1998).

[6] N. Iwama *et al.*, Appl. Phys. Lett. **54**, 502 (1989).

[7] Y. Liang, These proceeding .

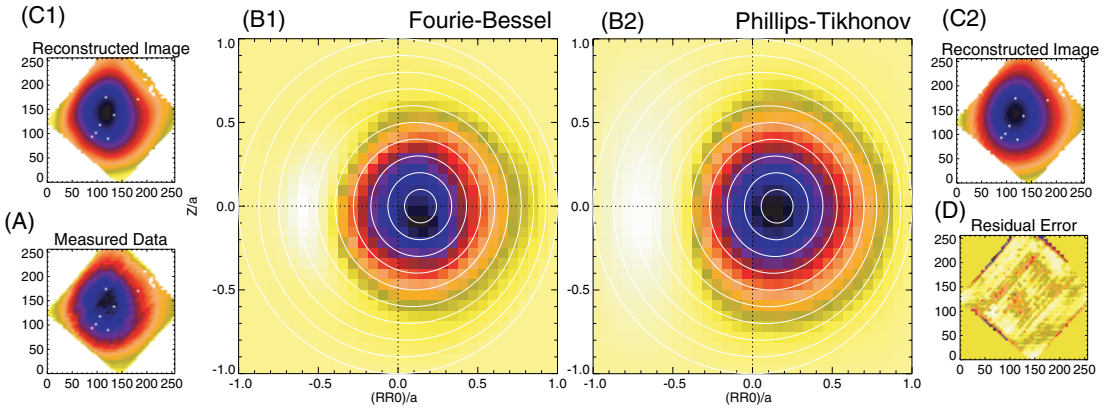

Fig.3: Tomographic reconstruction using two methods. (A) measured data. (B1) and (B2) reconstructed radiation profiles by FB and PT, respectively, (C1) and (C2) tangentially viewing image assuming radiation profile (B1) and (B2). (D) gives the residual error obtained by (A) and (C2).

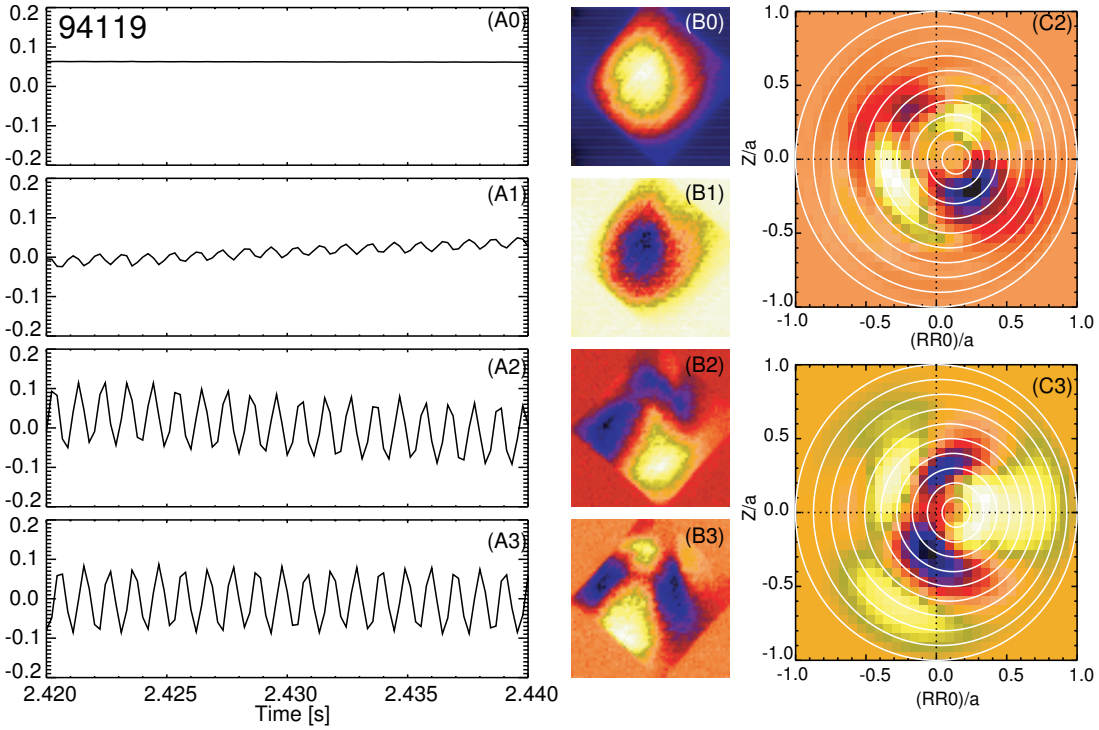

Fig.4: Choronos(A0-A3) and Topos(B0-B3) for the DED experiments. Tomographic reconstruction using FB expansion of (B2) and (B3) are also shown in (C2) and (C3), respectively.